AIChE

Solid–Liquid Equilibria of Multicomponent Lipid Mixtures Under CO_2 Pressure: Measurement and Thermodynamic Modeling

K. Vezzù and A. Bertucco
Dept. of Chemical Engineering, University of Padova, 35131 Padova, Italy

F. P. Lucien
School of Chemical Sciences and Engineering, The University of New South Wales, UNSW Sydney, NSW 2052, Australia

DOI 10.1002/aic.11543
Published online July 11, 2008 in Wiley InterScience (www.interscience.wiley.com).

A method for evaluating solid–liquid equilibria of mixtures of lipids and carbon dioxide (CO_2) under pressure is developed and presented in this article. Experimental measurements by high-pressure differential scanning calorimetry (DSC) are performed to determine solid–liquid transition temperatures as a function of composition. These data are used to develop a simplified approach for thermodynamic modeling, that is, correlation and prediction, of the solid–liquid equilibria. The model requires fewer pure component properties in comparison with cubic equations of state: the solid-state fugacity is determined with reference to the subcooled liquid state whereas regular solution theory is applied for the calculation of liquid-phase activity coefficients. Application of the model is demonstrated for mixtures of ceramide 3A and cholesterol in compressed CO_2 in the range of pressure from 0.1 to 6.1 MPa. A satisfactory correlation of solid–liquid equilibria is obtained for binary systems consisting of either the lipid mixture or one lipid in compressed CO_2. With the fitted binary interactions parameters, the eutectic temperature of the ternary mixture is predicted to within 1°C of the experimental value in the range of pressure considered. The proposed evaluation method looks sufficiently accurate for representing multiphase equilibria of lipid mixtures in compressed CO_2 and has direct application to gas-assisted micronization processes such as PGSS (Particles from Gas-Saturated Solution). © 2008 American Institute of Chemical Engineers *AIChE J,* 54: 2487–2494, 2008
Keywords: solid–liquid equilibria, lipids, carbon dioxide, differential scanning calorimetry, gas saturated solutions, PGSS

Introduction

Solid lipid nanoparticles (SLN) are colloidal dispersions that have attracted increasing attention in the production of pharmaceutical and cosmetic formulations.[1–3] Such materials are employed as drug carrier systems and permit a more controlled and targeted release of the active drug. The conventional techniques for producing SLN include high pressure homogenization, high shear homogenization, and ultrasound.[4] More recently, the gas-assisted micronization process known as Particles from Gas-Saturated Solutions (PGSS)[5] has been considered for the preparation of SLN.[6,7]

The PGSS process exploits the melting point depression of a solid in the presence of a compressed gas. Under these conditions, the molten solid becomes saturated with appreciable quantities of the gas. The solution is expanded through a fine nozzle where it undergoes rapid cooling because of the Joule-Thomson effect. Simultaneously, the evaporation of the

Correspondence concerning this article should be addressed to A. Bertucco at alberto.bertucco@unipd.it.

gas from the solution leads to the formation of very small solid particles. Carbon dioxide is the gas of choice in most applications because of its benign characteristics and low cost. The PGSS process is well suited to lipids because they can be melted at relatively mild operating temperatures and CO_2 exhibits high solubility in the liquid phase.

The solid–liquid-vapor (SLV) coexistence curve of a solid in a compressed gas is of primary importance in assessing the feasibility of PGSS and the selection of appropriate operating conditions.[8–10] Future application of the PGSS process for producing SLN is expected to involve lipid mixtures. Multiphase equilibria of lipid mixtures in compressed gases are therefore of growing interest. In the simplest case of a binary solid mixture, the pressure-dependence of the eutectic melting temperature is represented by the solid 1-solid 2-liquid-vapor (S_1S_2LV) coexistence curve.[11–13] In a similar manner to pure solids, the eutectic temperature may be significantly reduced in the presence of high pressure CO_2. Thermodynamic modeling of this complex phenomenon is a challenging task in view of the highly asymmetric nature of the mixtures.

Cubic equations of state are commonly used to represent SLV equilibria of solids in compressed gases.[8,14,15] While the liquid and vapor fugacity coefficients are calculated with the equation of state, a different approach is followed for the solid-state, which is assumed to be pure. A hypothetical subcooled liquid is normally used as the reference state for evaluating the solid-state fugacity.[16] The temperature, pressure, and phase compositions are obtained from simultaneous solution of the various fugacity equations. The pure component properties required in the equation of state are the critical temperature, critical pressure, and acentric factor. For lipids and other biomaterials, these properties are usually unavailable or indeterminate because of thermal degradation of the materials below the critical point. Furthermore, estimation methods for these properties are known to be less reliable for solids compared with liquids.

The objective of this work is to develop a simplified approach to modeling multiphase equilibria of lipid mixtures in compressed CO_2. Here we retain the subcooled liquid as the reference state for the solid-phase fugacity. The advantage of this method is that only the heat of fusion and the melting temperature of the solid are required. Both of these properties can be determined directly from differential scanning calorimetry (DSC). For the vapor phase, we note that the solubility of heavy components in compressed CO_2 rarely exceeds 1 mol %.[17] Since the vapor phase is of minor importance in the PGSS process, it is convenient to assume that the vapor phase is pure CO_2. Carbon dioxide is a well-characterized gas and any number of equations of state can be used to evaluate the fugacity. Finally, regular solution theory is applied for the calculation of activity coefficients to quantify nonideality in the liquid phase. The use of activity coefficients rather than fugacity coefficients eliminates the need for critical properties of the solids.

Ceramides, fatty acids, and cholesterol are examples of epidermal lipids that find application in the preparation of SLN, because they represent an innovative "dermatological ingredient" for topical formulation. These lipids, in fact, have been demonstrated to be successful in treatment of common skin diseases, involving barrier deficiencies, such us atopic dermatitis, psoriasis, xerosis, and pruritous in elderly patients.[18] In the present study, we examine the solid–liquid phase behavior of mixtures of ceramide 3A and cholesterol in CO_2 in the range of pressure from 0.1 to 6.1 MPa. For thermodynamic modeling purposes, solid–liquid equilibrium data are reported for the pure lipids and their mixtures in CO_2. Differential scanning calorimetry is used to determine solid–liquid transition temperatures as a function of composition. This technique has been reported previously for constructing solid–liquid phase diagrams for lipid mixtures at atmospheric pressure.[19–22] Typically, lipid mixtures are described by eutectic-type phase diagrams. To the best of our knowledge, the use of this technique for lipid mixtures in high pressure CO_2 has not been reported.

Thermodynamic Modeling

Binary SL equilibria: 2 lipids

The melting behavior of two lipids at ambient pressure was modeled as the solubility of a solid (2) in a liquid solvent (1). If the solid phase is assumed to be pure, the equilibrium distribution of the solute between the two phases is represented as:

$$f_2^s = \gamma_2 x_2 f_2^l \tag{1}$$

where f_2^s is the fugacity of the pure solid, γ_2 is the liquid-phase activity coefficient, x_2 is the liquid-phase mole fraction, and f_2^l is the standard-state fugacity of the solute as a hypothetical subcooled liquid. The ratio of the fugacities in Eq. 1, at a given temperature (T), is given by[16]:

$$\ln\frac{f_2^s}{f_2^l} = -\frac{\Delta H_t}{RT_t}\left(\frac{T_t}{T}-1\right) + \frac{\Delta c_p}{R}\left(\frac{T_t}{T}-1\right) - \frac{\Delta c_p}{R}\ln\frac{T_t}{T} \tag{2}$$

$$\Delta c_p = c_p^l - c_p^s \tag{3}$$

where ΔH_t is the enthalpy of fusion at the triple-point temperature (T_t), c_p^l and c_p^s are the heat capacities of the subcooled liquid and solid, respectively. It is common practice to substitute T_t with the normal melting temperature (T_m) and to replace ΔH_t with the enthalpy of fusion (ΔH_m) at T_m. Further simplification to Eq. 2 can be made by noting that the terms containing Δc_p are approximately equal. The solubility of the solid in the solvent may therefore be expressed as:

$$\ln \gamma_2 x_2 = -\frac{\Delta H_m}{RT_m}\left(\frac{T_m}{T}-1\right) \tag{4}$$

The liquid-phase activity coefficient of the solute was estimated using the Scatchard-Hildebrand relation:

$$\ln\gamma_2 = \frac{v_2^l[(\delta_1-\delta_2)^2 + 2l_{12}\delta_1\delta_2]\Phi_1^2}{RT} \tag{5}$$

$$\text{with} \quad \Phi_1 = \frac{x_1 v_1^l}{x_1 v_1^l + x_2 v_2^l} \tag{6}$$

where v_2^l is the molar volume of the subcooled liquid, δ_1 and δ_2 are the solubility parameter of the solvent and of the subcooled liquid, respectively, Φ_1 is the volume fraction of

Table 1. Estimated Molar Volumes and Solubility Parameters for Ceramide 3A, Cholesterol, and Carbon Dioxide at 25°C

Component	Molar Volume (cm^3/mol)	Solubility Parameter ($J^{1/2}/cm^{3/2}$)
Ceramide 3A	588*	20.1†
Cholesterol	383*	19.0†
CO_2	55*	12.3‡

*Average of the values calculated from the Hoy method and the Fedors method.[22]
†Calculated using the Hoftyzer and Van Krevelen method.[22]
‡Value shown is for CO_2 as a hypothetical liquid.[16]

solvent and l_{12} is the binary interaction parameter. Although solubility parameters are functions of temperature, the numerator in Eq. 5 displays a weak dependence on temperature. Any convenient temperature may be used to evaluate the molar volume and solubility parameter, provided that the same temperature is used for both components.

It should be noted that Eq. 5 was developed from regular solution theory for pure components that are normally liquids. The lipids of interest here are solids in pure form at the solution temperatures. Prausnitz et al.[16] describe a thermodynamic cycle by which values of v and δ can be calculated for a solid in the form of a hypothetical subcooled liquid. However, the additional thermal and volumetric properties required for the calculation are unavailable in this case. Here we introduce an empirical modification to Eq. 5 by employing values of v and δ for each lipid in the solid state at 25°C. Adjustment to the liquid-phase activity coefficient is made with l_{12}. Molar volumes and solubility parameters were estimated using the group contribution methods described by Van Krevelen.[23] A list of the pure component parameters used in the modeling of solid–liquid equilibria is presented in Table 1.

The use of a binary interaction parameter in Eq. 5 represents an empirical modification for correcting deviations from the geometric-mean assumption in regular solution theory. This modification permits regular solution theory to be extended to asymmetric mixtures consisting of CO_2 and a heavy component whose molar volume is substantially larger than that of the gas. Further extension to mixtures containing moderately polar components can be made by employing an extended solubility parameter. The extended solubility parameter is divided into separate contributions from nonpolar (dispersion) forces, polar forces, and hydrogen bonding. The Hoftyzer and Van Krevelen method[23] expresses the solubility parameter as:

$$\delta_{\text{total}}^2 = \delta_{\text{d}}^2 + \delta_{\text{p}}^2 + \delta_{\text{h}}^2 \tag{7}$$

where the subscripts d, p, and h indicate the contributions from dispersion, polar, and hydrogen-bonding forces. This method has been widely applied to polymers and is readily extended to heavy components such as lipids.

Equations 4–6 provide a means of calculating the composition of the liquid phase in equilibrium with excess solid 2 at various temperatures. By reversing the subscripts, the same equations can be used to determine the liquid-phase composition in the presence of excess solid 1. In this way, a T–x phase diagram can be constructed depicting regions of SL equilibria. The intersection of the two branches of the T–x diagram marks the eutectic point at which three phases (S_1S_2L) are in equilibrium. According to the phase rule for nonreacting systems, there is one degree of freedom for a binary system with three coexisting phases. For a specified pressure (P), the eutectic temperature (T_{eut}) and the corresponding liquid-phase composition are therefore fixed. The two unknowns (T_{eut}, x_{eut}) are determined by simultaneous solution of the two solubility equations (one for each solid).

The value of l_{12} was regressed from experimental T–x data. The experimental values of liquid-phase composition were used to generate calculated values of the solution temperature via Eqs. 4–6. The same value of interaction parameter was used for each branch of the T–x diagram ($l_{12} = l_{21}$). The optimum value of l_{12} was obtained by minimizing the sum of squared deviations (SSD) with respect to temperature:

$$\text{SSD} = \sum_{i=1}^{M} (T_{\text{calc}} - T_{\text{exp}})^2 \tag{8}$$

where M is the number of data points, T_{calc} and T_{exp} are the calculated and experimental values of temperature, respectively.

Binary SLV equilibria: 1 lipid + CO_2

The melting behavior of a lipid in the presence of high pressure CO_2 was modeled using a procedure similar to that described earlier. In this case, we consider the solubility of a gas (2) in a liquid solvent (1). If the gas phase is assumed to be pure, the equilibrium distribution of CO_2 between the two phases is represented as:

$$f_2^{\text{g}} = \gamma_2 x_2 f_2^{\text{l}} \tag{9}$$

where f_2^{g} is the fugacity of pure CO_2, γ_2 is the liquid-phase activity coefficient, x_2 is the liquid-phase mole fraction, and f_2^{l} is the standard-state fugacity of CO_2 as a hypothetical liquid. Regular solution theory (Eqs. 5 and 6) was again applied for the liquid-phase activity coefficient. The required molar volume and solubility parameter for CO_2 as a hypothetical liquid at 25°C are listed in Table 1. The fugacity of CO_2 as a hypothetical liquid was evaluated as follows:

$$f_2^{\text{l}}(T,P) = f_{2,1\text{atm}}^{\text{l}}(T)\ \exp\left[\frac{v_2^{\text{l}}(P-1.013)}{RT}\right] \tag{10}$$

Values of the fugacity at 1 atm ($f_{2,1\text{atm}}^{\text{l}}$) are presented in a corresponding-states plot elsewhere.[16] The fugacity of pure CO_2 was calculated from the equation of state proposed by Sievers.[24] The solubility of CO_2 in the molten lipid as a function of pressure can therefore be represented as:

$$\frac{1}{\gamma_2 x_2} = \frac{f_{2,1\text{atm}}^{\text{l}}}{f_2^{\text{g}}}\ \exp\left[\frac{v_2^{\text{l}}(P-1.013)}{RT}\right] \tag{11}$$

For a binary system with SLV coexisting phases, there is one degree of freedom. The melting temperature of the solid and the liquid-phase composition are fixed once a value for

pressure is specified. Simultaneous solution of Eqs. 4 (solid solubility) and 11 (gas solubility) yields the calculated melting temperature and liquid-phase composition. The value of l_{12} was regressed from experimental melting temperatures obtained at different pressures. The optimum value of l_{12} was obtained by minimizing the SSD with respect to temperature (Eq. 8).

Ternary SLV equilibria: 2 lipids + CO_2

The melting behavior of two lipids in the presence of high-pressure CO_2 was modeled using Eq. 4 to represent the dissolution of each solid in the liquid phase. This approach again assumes that each solid phase remains pure. Equation 11 was used to calculate the solubility of CO_2 in the molten lipids. The use of regular solution theory to describe the liquid-phase activity coefficient can be generalized for mixtures containing more than two components as follows:

$$RT\ \ln\gamma_k = v_k \sum_{i=1}^{N}\sum_{j=1}^{N} \Phi_i\Phi_j\left[D_{ik} - \frac{1}{2}D_{ij}\right] \tag{12}$$

$$D_{ij} = (\delta_i - \delta_j)^2 + 2l_{ij}\delta_i\delta_j \tag{13}$$

$$\Phi_j = \frac{x_j v_j}{\sum_{i=1}^{N} x_i v_i} \tag{14}$$

where N is the number of components and for every component i, $l_{ii} = D_{ii} = 0$. No new interaction parameters are required in the ternary system. Thus once the respective binary interaction parameters are obtained the model becomes predictive for multicomponent systems.

At the eutectic point, four phases (S_1S_2LV) are in equilibrium and there is one degree of freedom. For a specified pressure, the eutectic temperature and the corresponding liquid-phase composition are therefore fixed. In this situation, there are three unknowns: T_{eut} and two composition variables. The required values are determined by simultaneous solution of the three solubility equations: Eq. 4 for each solid and Eq. 11 for the gas solubility.

Experimental

Materials

Ceramide 3A[25] (*N*-linoeoyl-phytosphingosine, 97%) and cholesterol ($C_{27}H_{46}O$, 99%, CAS 57-88-5) were obtained from Unifarco. The lipids were used as received without further purification. Carbon dioxide (99.95%) was purchased from Sapio.

Preparation of lipid mixtures

Small batches of lipid mixtures (100–150 mg) were prepared by placing the required amounts of solid Ceramide 3A and cholesterol into a glass container. The accuracy of weighing was ± 0.0001 g. The mixtures were melted in an air oven at 140°C and maintained at this temperature for a period of 5 min. After briefly stirring the molten lipids, they were allowed to cool to room temperature. The solidified mixture was manually fractured with a metal spatula and ground into a fine powder. The composition of the mixtures is expressed in terms of the mole fraction of Ceramide 3A (x_{cer}).

DSC measurements

Differential scanning calorimetry was performed using a TA Instruments calorimeter (model Q10P). This instrument is equipped with a high pressure cell that enables measurements to be performed in the presence of CO_2 up to a maximum operating pressure of 7 MPa. An amount of 5–10 mg of mixture (or pure lipid) was weighed into an aluminium pan and placed in the calorimeter. For experiments involving CO_2, the cell was pressurized to the desired operating pressure prior to heating of the sample. A continuous flow of CO_2 was maintained through the cell during the heating cycle. The sample was heated from 25 to 150°C at a rate of 1°C/min. DSC measurements for a given sample were performed at least twice.

The influence of sample mass and heating rate on the melting temperature was also considered for experiments at ambient pressure. The uncertainty in the melting temperature for a given mixture was generally less than 0.5°C for the stated range of sample mass and for heating rates in the range of 0.5–1°C/min. At higher pressures, the uncertainty in the melting temperature was greater (<1°C) because of fluctuations in pressure (<0.1 MPa) during the heating cycle.

Results and Discussion

Binary SL equilibria: 2 lipids

Typical thermograms for the pure lipids and their mixtures at 0.1 MPa are presented in Figure 1. Beginning with pure Ceramide 3A, the thermogram reveals the onset of one large endothermic peak at around 120°C and a smaller endothermic peak at 80°C. The smaller peaks is probably a solid–solid phase transition associated with polymorphism of the lipid.[25] In the case of cholesterol, only a single endothermic peak is visible in the same range of temperature. In this study, the melting temperature of a pure lipid is assigned the value at the minimum of the main peak.[20] The melting temperatures and enthalpies of fusion obtained for the pure lipids are presented in Table 2. Some reference values are also shown in the table for comparative purposes.

The thermograms for the lipid mixtures generally reveal two main endothermic peaks. The temperature at the minimum of the first peak remains almost constant whereas that for the second peak increases as the mole fraction of cholesterol increases. The temperature at a peak minimum is assumed to represent the point at which the last trace of a given crystalline phase disappears. Proceeding on this basis, the phase boundaries of the solid–liquid phase diagram can be constructed as shown in Figure 2. The resulting diagram is similar to that for a eutectic-type system. The mean value of the eutectic temperature is 106°C and the eutectic composition is close to 40 mol % Ceramide 3A, in view of the single peak observed at this composition. Previous studies have also reported eutectic-type phase diagrams for mixtures of other Ceramide 3A forms with cholesterol or fatty acids.[20–22]

For a mixture at the eutectic composition, both solids melt completely before further increases in temperature occur. For mixtures on either side of this point, there are two regions of

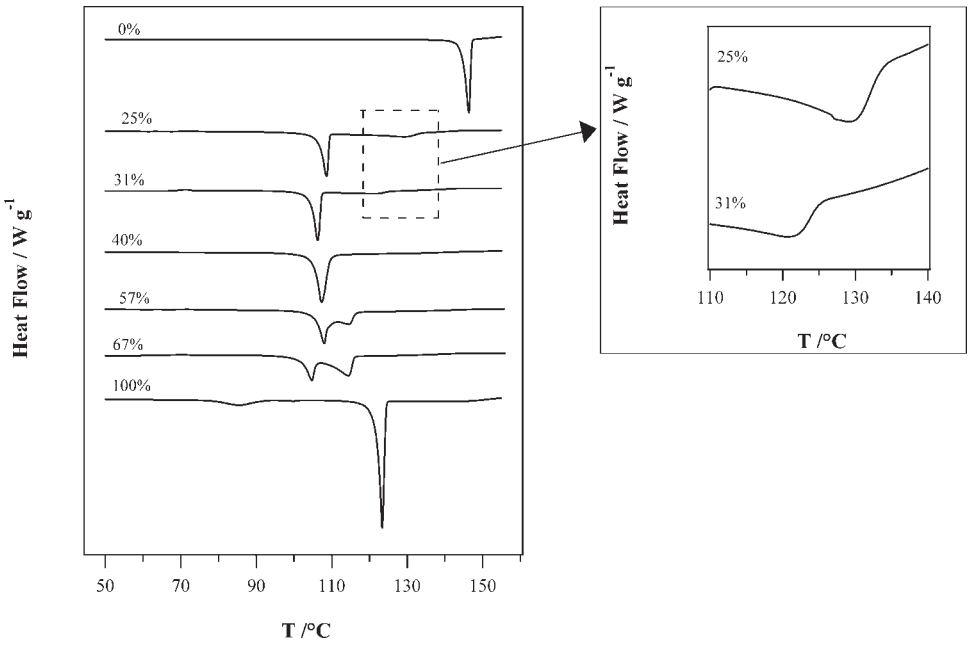

Figure 1. Typical thermograms for the pure lipids and their mixtures at 0.1 MPa.

The percentage figure denotes the composition of ceramide 3A in the mixture.

solid–liquid equilibria in which only one solid melts completely. Accordingly, the transition enthalpy per mole of mixture at the eutectic temperature exhibits a maximum value at the eutectic composition.[20] The experimental values of the transition enthalpies obtained at T_{eut} are presented as a function of composition in Figure 3. For the 57% and 67% mixtures, the two peaks were resolved into separate peaks, using Igor Pro 5.04B software, before the calculation of the transition enthalpy. Based on the data in Figure 3, the estimated eutectic composition is slightly higher than 40 mol % Ceramide 3A ($x_{eut} \sim 0.46$).

Correlation of the solid–liquid equilibria using regular solution theory is also presented in Figure 2. It can be seen that there is close agreement between the model and the experimental data. The average absolute relative deviation (AARD) with respect to the calculated temperature is 2% and the fitted value of l_{12} is -0.0002 (Table 3). Estimation of molar volumes and solubility parameters in the solid state at 25°C clearly yields a satisfactory outcome in this analysis. The relatively small value for l_{12} is attributed to the similar values of δ for the lipids, a result that implies near-ideal solution behavior ($\gamma \sim 1$). Simultaneous solution of the solubility equations with the fitted value of l_{12} produces the following coordinates for the eutectic point: $T_{eut} = 105.7$°C, $x_{eut} = 0.47$. The predicted eutectic composition is consistent with the value estimated from analysis of transition enthalpies (Figure 3).

Table 2. Melting Temperatures and Enthalpies of Fusion for Ceramide 3A and Cholesterol

	T_m (°C)		ΔH_f (kJ/mol)	
Components	This Work	Reference	This Work	Reference
Ceramide 3A	124.0	–	50.8	–
Cholesterol	146.9	147.1[25] 149.2[26]	20.0	29.9[25] 28.4[26]

Binary S-L-V equilibria: 1 lipid + CO_2

Typical thermograms for Ceramide 3A in the presence of high pressure CO_2 are shown in Figure 4. At a pressure of 6.1 MPa, the melting point for Ceramide 3A decreases by

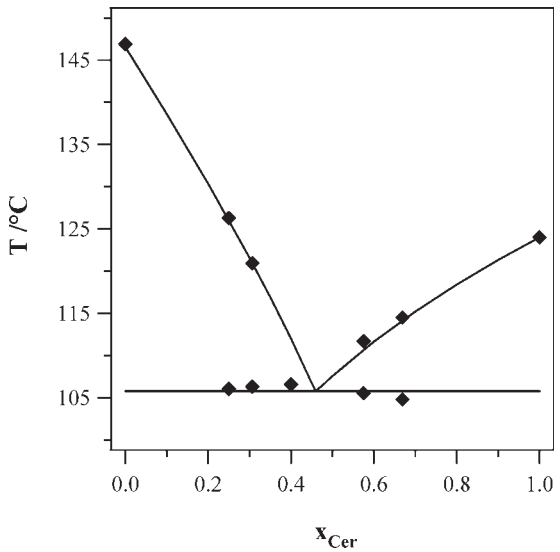

Figure 2. Solid–liquid phase diagram for ceramide 3A-cholesterol at 0.1 MPa.

The solid line represents the correlation of the data with the regular solution model.

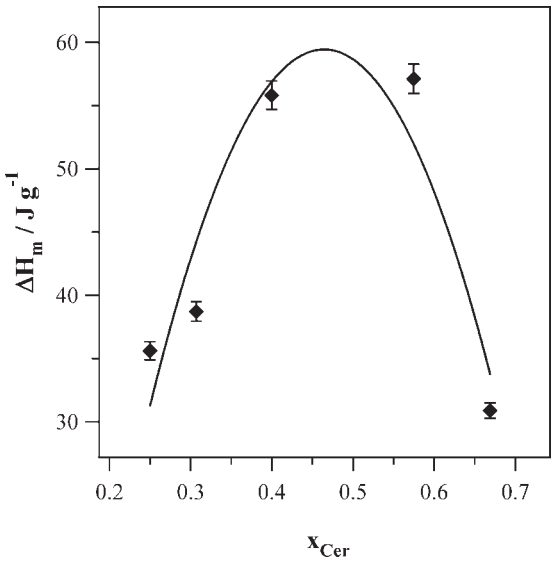

Figure 3. Experimental values of the transition enthalpies obtained at T_{eut} as a function of composition.

The solid line denotes the curve of best fit.

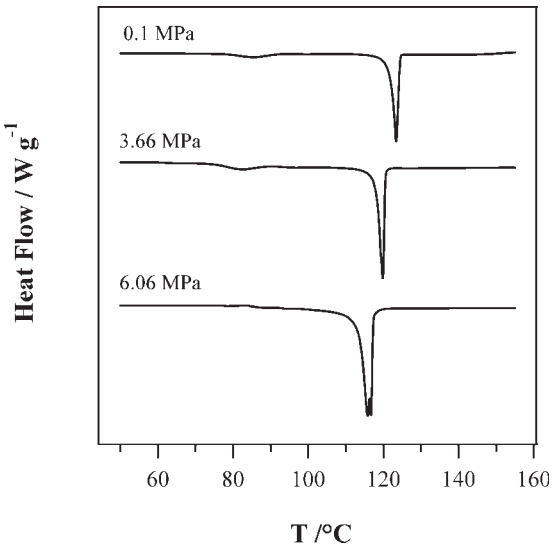

Figure 4. Typical thermograms for pure ceramide 3A in CO_2 at various pressures.

8°C in comparison with the normal value. The corresponding reduction for cholesterol is 10°C (thermograms not shown). A close examination of the thermogram for Ceramide 3A at 6.1 MPa reveals the appearance of two unresolved peaks in the main endothermic peak whereas the smaller endothermic peak observed in Figure 1 is much less evident. This suggests that pressure exerts some influence over the formation of Ceramide 3A polymorphs. Spilimbergo et al.[9] have observed a similar effect in the melting and crystallizations curves of a triglyceride in the presence of compressed CO_2.

The solubility parameter for CO_2 (Table 1) is much lower than that for either lipid and greater deviation from an ideal solution is expected. This is illustrated in Figure 5, which depicts the *P–T* projection of the SLV coexistence curve for each lipid. For an ideal solution, the correlation of the melting temperatures is unsatisfactory. With the fitted interaction parameters shown in Table 3, the correlation of the data is significantly improved. The AARDs with respect to temperature are less than 1% for both Ceramide 3A and cholesterol.

A near-linear dependence is observed between pressure and the lipid melting temperature in Figure 5. At higher pressures this is not expected to be the case. The SLV coexistence curve often exhibits a temperature minimum, beyond which the melting temperature usually increases with pressure.[8,28,29] Because of the pressure limitation of the DSC unit, we were unable to generate SLV data beyond 7.0 MPa.

Table 3. Optimized Values of l_{ij} ($=l_{ji}$) for the Estimation of the Liquid-Phase Activity Coefficient Using Regular Solution Theory

Binary System	l_{ij}	SSD	AARD (%)
Ceramide-cholesterol	−0.00021	3.07	2.1
Ceramide-CO_2	−0.095	0.18	0.2
Cholesterol-CO_2	−0.0025	0.19	0.1

It is therefore difficult to assess whether the regular solution model can accurately describe the temperature minimum in the SLV curve. Nonetheless, the regular solution model presents certain simplifying features and these are highlighted more clearly in the next section.

Ternary SLV equilibria: 2 lipids + CO_2

The constructed solid–liquid phase boundaries for the lipid mixtures in the presence of CO_2 are shown in Figure 6. Mixture composition is expressed on a CO_2-free basis. The thermograms under these conditions exhibit similar characteristics to those shown in Figure 1 and are not reproduced here. At both pressures, the phase diagram again exhibits the features of a eutectic system. The eutectic temperature decreases

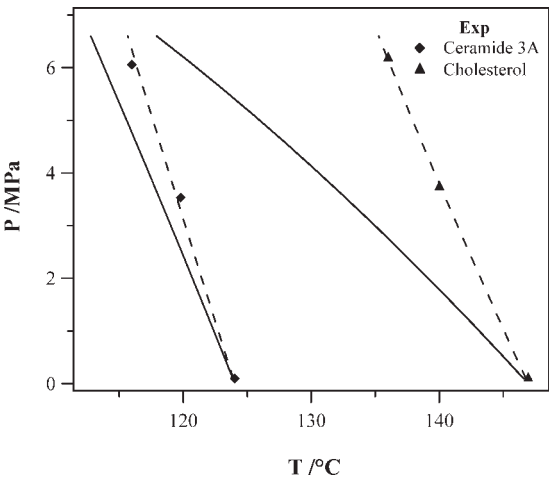

Figure 5. *P–T* projection of the SLV coexistence curves for the pure lipids in CO_2.

The solid lines represent correlation of the data assuming an ideal solution ($\gamma = 1$). The dashed lines are the correlation of the data with the fitted binary interaction parameters.

by around 9°C at a pressure of 6.1 MPa. Only a single peak was detected in the DSC thermogram for the 40 mol % mixture at both pressures, indicating that the eutectic composition (CO_2-free basis) is not strongly influenced by pressure in the range considered.

The calculated solid–liquid equilibria in Figure 6 show excellent agreement with the experimental data. It should be noted that the ternary phase equilibrium data are predicted only from pure component properties and the binary interaction parameters fitted on binary lipid-CO_2 data (Table 3). A comparison between the predicted and experimental values of T_{eut} is given in Table 4, along with the calculated liquid-phase composition. In general, the model predicts the eutectic temperature to within 1°C of the mean experimental value. Determination of the solubility of CO_2 in the molten lipids is not possible with the DSC method used in this study. The modeling results, however, clearly indicate the presence of significant quantities of CO_2 in the liquid phase. The estimated solubility at the eutectic point at 6.1 MPa is 25 mol % CO_2, thus highlighting the potential utility of PGSS for the preparation of SLN.

A cubic equation of state can also be used to predict the ternary solid–liquid equilibria once the required interaction parameters have been fitted from binary data. However, the use of regular solution theory to model the liquid phase represents an easier approach, mainly because of the relative simplicity of the activity coefficient expression. Calculation of the activity coefficient also requires fewer pure component properties of the lipids compared with the corresponding fugacity coefficient equation. The molar volumes and solubility parameters of the lipids used in this work were estimated using group contribution methods originally proposed for solid polymers.[23] The accuracy of the modeling results in conjunction with the relatively small values of the interaction parameters confirm that this approach is satisfactory for the system of interest.

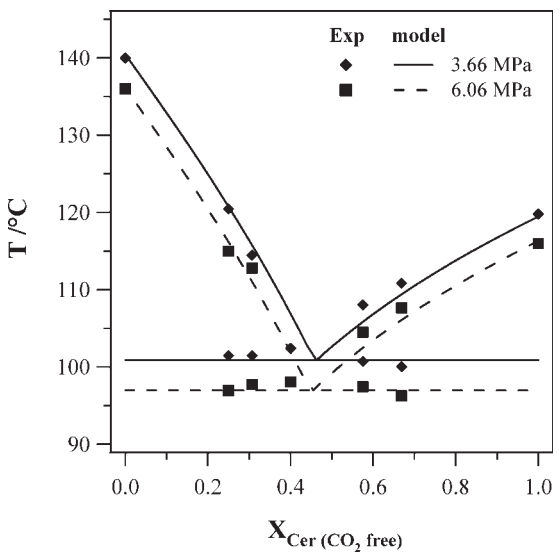

Figure 6. Solid–liquid phase diagrams for ceramide 3A-cholesterol mixtures in CO_2.

Composition is expressed on a CO_2-free basis.

Table 4. Predicted Eutectic Points Using Regular Solution Theory

P (MPa)	T_{eut}^{exp} (°C)	T_{eut} (°C)	x_{cer}	x_{chol}	x_{CO_2}
0.1	105.9	105.7	0.47	0.53	–
3.66	101.2	100.8	0.39	0.46	0.15
6.06	97.2	96.8	0.34	0.41	0.25

Conclusions

A general and simplified method for evaluating solid–liquid equilibria of mixtures of lipids and carbon dioxide (CO_2) under pressure was developed. The method is based on experimental measurements by high-pressure differential scanning calorimetry (DSC) and thermodynamic modeling with regular solution theory. It allows a simple correlation of binary data and an accurate prediction of ternary solid–liquid coexistence curves. Measurements performed on mixtures of ceramide 3A and cholesterol pressurized with CO_2 indicated that, under the influence of compressed CO_2, the eutectic temperature decreased by around 9°C at a pressure of 6.1 MPa. The proposed thermodynamic model provided a satisfactory correlation of solid–liquid equilibria for binary systems consisting of either the lipid mixture or one lipid in compressed CO_2. With the fitted binary interactions parameters, the eutectic temperature of the ternary mixture was predicted to within 1°C of the experimental value in the range of pressure considered. Regular solution theory complemented with a few experimental determinations offers a simpler approach to modeling multiphase equilibria of lipid mixtures in compressed CO_2 and looks valuable in view of the development of new and emerging solvent-free micronization processes such as PGSS (Particles from Gas-Saturated Solution).

Acknowledgments

The support of the Italian Minister of Research (MIUR) under PRIN 05 program is gratefully acknowledged.

Literature Cited

1. Wissing SA, Kayser O, Muller RH. Solid lipid nanoparticles for parenteral drug delivery. *Adv Drug Deliv Rev*. 2004;56:1257–1272.
2. Hu JH, Johnston KP, Williams RO. Nanoparticle engineering processes for enhancing the dissolution rates of poorly water-soluble drugs. *Drug Dev Ind Pharm*. 2004;30:233–245.
3. Wissing SA, Lippacher A, Müller RH. Investigations on the occlusive properties of solid lipid nanoparticles (SLN). *J Cosmet Sci*. 2001;52:313–324.
4. Mehnert W, Mäder K. Solid lipid nanoparticles production, characterization and applications. *Adv Drug Deliv Rev*. 2001;47:165–196.
5. Jung J, Perrut M. Particle design using supercritical fluids. Literature and patent survey. *J Supercrit Fluids*. 2001;20:179–219.
6. Elvassore N, Flaibani M, Bertucco A, Caliceti P. Thermodynamic analysis of micronization processes from gas-saturated solution. *Ind Eng Chem Res*. 2003;42:5924–5930.
7. Elvassore N, Flaibani M, Vezzu' K, Bertucco A, Caliceti P. Lipid system micronization for pharmaceutical applications by PGSS techniques. Proceedings of the 6th International Symposium on Supercritical Fluids, Versailles, France, April 28–30, 2003.
8. Bertakis E, Lemonis I, Katsoufis S, Voutsas E, Dohrn R, Magoulas K, Tassios D. Measurement and thermodynamic modeling of solid-liquid-gas equilibrium of some organic compounds in the presence of CO_2. *J Supercrit Fluids*. 2007;41:238–245.

9. Spilimbergo S, Luca G, Elvassore N, Bertucco A. Effect of high-pressure gases on phase behaviour of solid lipids. *J Supercrit Fluids*. 2006;38:289–294.
10. Fischer K, Wilken M, Gmehling J. The effect of gas pressure on the melting behavior of compounds. *Fluid Phase Equilib*. 2003;210: 199–214.
11. Zhang D, Cheung A, Lu C-Y. Multiphase equilibria of binary and ternary mixtures involving solid phase (s) at supercritical fluid conditions. *J Supercrit Fluids*. 1992;5:91–100.
12. Lemert RM, Johnston KP. Solubilities and selectivities in supercritical fluid mixtures near critical end points. *Fluid Phase Equilib*. 1990;59:31–55.
13. White GL, Lira CT. Four-phase (solid-solid-liquid-gas) equilibrium of two ternary organic systems with carbon dioxide. In: Johnston KP, Penninger JML, editors. *Supercritical Fluid Science and Technology*. Washington: American Chemical Society, 1989:111–120.
14. Diefenbacher A, Türk M. Phase equilibria of organic solid solutes and supercritical fluids with respect to the RESS process. *J Supercrit Fluids*. 2002;22:175–184.
15. Kikic I, Lora M, Bertucco A. A thermodynamic analysis of three-phase equilibria in binary and ternary systems for applications in rapid expansion of a supercritical solution (RESS), particles from gas-saturated solutions (PGSS), and supercritical antisolvent (SAS). *Ind Eng Chem Res*. 1997;36:5507–5515.
16. Prausnitz JM, Lichtenthaler RN, de Azevedo EG. Solubility of gases in liquids. and solubility of solids in liquids. In: Prausnitz JM, Lichtenthaler RN, de Azevedo EG, editors. *Molecular Thermodynamics of Fluid-Phase Equilibria*, 2nd ed. Englewood, Cliff: Prentice Hall, 1986:389–396, 415–438.
17. Lucien FP, Foster NR. Solubilities of solid mixtures in supercritical carbon dioxide: a review. *J Supercrit Fluids*. 2000;17:111–134.
18. Man M-Q, Feingold KR, Thornfeldt CR, Elias PM. Optimization of physiological lipid mixtures for barrier repair. *J Invest Dermatol*. 1996;106:1096–1101.
19. Teixeira ACT, Gonçalves da Silva AMPS, Fernandes AC. Phase behaviour of stearic acid-stearonitrile mixtures: a thermodynamic study in bulk and at the air-water interface. *Chem Phys Lipids*. 2006;144:160–171.
20. Ohta N, Hatta I. Interaction among molecules in mixtures of ceramide/stearic acid, ceramide/cholesterol and ceramide/stearic acid/cholesterol. *Chem Phys Lipids*. 2002;115:93–105.
21. Neubert R, Rettig W, Wartewig S, Wegener M, Wienhold A. Structure of stratum corneum lipids characterized by FT-raman spectroscopy and DSC. II. Mixtures of ceramides and saturated fatty acids. *Chem Phys Lipids*. 1997;89:3–14.
22. Wegener M, Neubert R, Rettig W, Wartewig S. Structure of stratum corneum lipids characterized by FT-raman spectroscopy and dsc. III. Mixtures of ceramides and cholesterol. *Chem Phys Lipids*. 1997; 88:73–82.
23. Van Krevelen DW. Cohesive properties and solubility. In: Van Krevelen DW, editor. *Properties of Polymers*, 3rd ed. Amsterdam: Elsevier,1990:189–225.
24. Sievers U. *Die Thermodynamischen Eigenschaften von Kohlendioxid*, 1st ed. Düsseldorf: VDI-Verlag, 1984.
25. Garidel P. Structural organization and phase behavior of a stratum corneum lipid analogue: ceramide 3A. *Phys Chem Chem Phys*. 2006;8:2265–2275.
26. Nichols G, Kweskin S, Frericks M, Reiter S, Wang G, Orf J, Carvallo B, Hillesheim D, Chickos J. Evaluation of the vaporization, fusion, and sublimation enthalpies of the 1-alkanols: the vaporization enthalpy of 1-, 6-, 7-, and 9-heptadecanol, 1-octadecanol, 1-eicosanol, 1-docosanol, 1-hexacosanol, and cholesterol at $T = 29815$ k by correlation gas chromatography. *J Chem Eng Data*. 2006;51:475–482.
27. Škerget M, Cretnik L, Knez Ž, Škrinjar M. Influence of the aromatic ring substituents on phase equilibria of vanillins in binary systems with CO_2. *Fluid Phase Equilib*. 2002;231:11–19.
28. Fukné-Kokot K, König A, Knez Ž, Škerget M. Comparison of different methods for determination of the S-L-G equilibrium curve of a solid component in the presence of a compressed gas. *Fluid Phase Equilib*. 2000;173:297–310.
29. van Miltenburg JC, van Genderen ACG, van den Berg GJK. Design improvements in adiabatic calorimetry: the heat capacity of cholesterol between 10 and 425 K. *Thermochim Acta*. 1998;319:151–162.

Manuscript received Dec. 26, 2007, and revision received Apr. 30, 2008.